Nanomechanical and Molecular Characterization of Aging in Dentinal Collagen

Journal of Dental Research
2022, Vol. 101(7) 840–847

DOI: 10.1177/00220345211072484
journals.sagepub.com/home/jdr

C.M.A.P. Schuh[1], C. Leiva-Sabadini[2], S. Huang[3], N.P. Barrera[4], L. Bozec[3], and S. Aguayo[2,5]

Abstract

Methylglyoxal (MGO) is an important molecule derived from glucose metabolism with the capacity of attaching to collagen and generating advanced glycation end products (AGEs), which accumulate in tissues over time and are associated with aging and diseases. However, the accumulation of MGO-derived AGEs in dentin and their effect on the nanomechanical properties of dentinal collagen remain unknown. Thus, the aim of the present study was to quantify MGO-based AGEs in the organic matrix of human dentin as a function of age and associate these changes with alterations in the nanomechanical and ultrastructural properties of dentinal collagen. For this, 12 healthy teeth from <26-y-old and >50-y-old patients were collected and prepared to obtain crown and root dentin discs. Following demineralization, MGO-derived AGEs were quantified with a competitive ELISA. In addition, atomic force microscopy nanoindentation was utilized to measure changes in elastic modulus in peritubular and intertubular collagen fibrils. Finally, principal component analysis was carried out to determine aging profiles for crown and root dentin. Results showed an increased presence of MGO AGEs in the organic matrix of dentin in the >50-y-old specimens as compared with the <26-y-old specimens in crown and root. Furthermore, an increase in peritubular and intertubular collagen elasticity was observed in the >50-y-old group associated with ultrastructural changes in the organic matrix as determined by atomic force microscopy analysis. Furthermore, principal component analysis loading plots suggested different "aging profiles" in crown and root dentin, which could have important therapeutic implications in restorative and adhesive dentistry approaches. Overall, these results demonstrate that the organic matrix of human dentin undergoes aging-related changes due to MGO-derived AGEs with important changes in the nanomechanical behavior of collagen that may affect diagnostic and restorative procedures in older people.

Keywords: atomic force microscopy, dentin, dental caries, advanced glycation end products, principal component analysis, enzyme-linked immunosorbent assay

Introduction

Currently, populations worldwide have experienced a rapid increase in life expectancy that has brought forward many challenges in diagnostics and treatment for older people (Prince et al. 2015). Elderly people are also likely to experience important oral pathologies, such as periodontal disease, dental caries (especially root caries), and oral candidiasis (Murray Thomson 2014). The process of aging is complex and involves an important number of biological and molecular changes in cells, tissues, and organs (DiLoreto and Murphy 2015; Sui et al. 2016); thus, it is essential to comprehend its impact on the pathogenesis of relevant oral diseases and restorative approaches.

Recently, much attention has been focused on investigating age-related changes in collagens (Gurav 2013; Ahmed et al. 2017), since they are the most abundant structural proteins in the body (Capella-Monsonís et al. 2018) and one of the main constituents of the organic matrix of dentin and periodontal tissues (Goldberg 2011). In modern restorative dentistry, dentinal collagen has become an important substrate for resin-dentin bonding and has been associated with the success or failure of the hybrid layer (Breschi et al. 2018). One of the most important age-associated changes in collagen results from the slow and irreversible accumulation of advanced glycation end products (AGEs; Nass et al. 2007).

[1]Centro de Medicina Regenerativa, Facultad de Medicina Clínica Alemana–Universidad del Desarrollo, Santiago, Chile
[2]Dentistry School, Faculty of Medicine, Pontificia Universidad Católica de Chile, Santiago, Chile
[3]Faculty of Dentistry, University of Toronto, Toronto, Canada
[4]Department of Physiology, Faculty of Biological Sciences, Pontificia Universidad Católica de Chile, Santiago, Chile
[5]Institute for Biological and Medical Engineering, Schools of Engineering, Medicine and Biological Sciences, Pontificia Universidad Católica de Chile, Santiago, Chile
A supplemental appendix to this article is available online.

Corresponding Author:
S. Aguayo, Dentistry School, Faculty of Medicine, Pontificia Universidad Católica de Chile, Avenida Libertador General Bernardo O'Higgins #340, Santiago, Santiago Province 3580, Chile.
Email: sebastian.aguayo@uc.cl

AGEs form sugar-residue crosslinks within the collagen and are often considered to have deleterious effects on the biophysical and biochemical properties of collagen-rich tissues. Some of the most medically relevant AGEs include glucosepane, pentosidine, and methylglyoxal (MGO)–derived AGEs (Gkogkolou and Böhm 2012). MGO is derived from glucose metabolism and can bind to lysine and arginine residues on the collagen molecule (Fessel et al. 2014; Wetzels et al. 2017). This process drives the formation of AGE-mediated adducts and crosslinks in a time-dependent manner; thus, the accumulation of AGEs is higher in tissues with slow collagen turnaround and in aged tissues (Ahmed et al. 2017). AGEs have been implied in a range of chronic diseases, and AGE-mediated protein modification is believed to be responsible for increasing the stiffness and fragility of collagen in human skin and bone (Snedeker and Gautieri 2014; Poundarik et al. 2015). To date, some studies have explored the effect of aging on the accumulation of certain AGEs in dentin, such as pentosidine (Shinno et al. 2016; Greis et al. 2018); at the macroscale, it has been shown that AGE accumulation in dentin results in altered mechanical properties, including higher tendencies to fracture under stress. However, not much is known regarding the accumulation of MGO-derived AGEs in dentin or the effect that these changes could generate on the ultrastructural and mechanical properties of dentinal collagen at the nanoscale level.

Major advances in the field of atomic force microscopy (AFM) in recent years have potentiated the nondestructive study of biological samples by combining topographic and nanomechanical assessment with nanoscale resolution (Dufrêne et al. 2021). By utilizing AFM, it is possible to not only characterize biological surfaces with submicron precision but also determine the elastic behavior of samples with nanoindentation-based approaches (Qian and Zhao 2018). The use of AFM for the study of collagens has allowed the exploration of their ultrastructural properties (Strange et al. 2017), including recent investigations of dentinal collagen from primary teeth in health and disease (Ibrahim et al. 2019). However, the accumulation of MGO-derived AGEs in the organic matrix of dentin that is associated with aging, as well as the impact of these AGEs on nanomechanical changes at the single collagen fibril level, has not yet been explored. Therefore, the aim of this study was to characterize the accumulation of MGO-based AGEs in the organic matrix of human dentin as a function of aging and to associate these changes with alterations in the nanomechanical and ultrastructural properties of dentinal collagen.

Materials and Methods

Tooth Specimen Collection

Ethical approval was obtained from the local University Ethics Committee at Pontificia Universidad Católica de Chile (180426002). Specimen collection was carried out at the School of Dentistry Clinical Center (CODUC; Santiago, Chile) following written informed consent. Twelve caries- and restoration-free teeth were employed for this study, as extracted due to orthodontic or rehabilitation treatments from systemically healthy individuals. Specimens were empirically divided into 2 age groups (<26 y and >50 y, $n = 6$ per group) to characterize aging-related changes. Upon collection, teeth were washed in phosphate buffer saline (PBS; 1×), mechanically debrided to remove remnants of periodontal tissue and dental pulp, and stored in 70% ethanol solution for 72 h. Specimens were then washed 3 times in PBS and stored in PBS at 4 °C before sectioning.

Dentin Section Preparation and Surface Demineralization

Following tooth debridement and washing, specimens were fully embedded in a dental acrylic resin (Marche Acrylics) and sectioned with a SP1600 hard tissue microtome (Leica Biosystems). From these sections, multiple dentin specimens from the crown and root (above and below the cementoenamel junction, respectively) were obtained with an individual thickness of 200 µm (Fig. 1A) and collected immediately for processing. For surface characterization, dentinal sections were demineralized by washing with a solution of 37% phosphoric acid (Sigma-Aldrich) for 30 s, rinsed with a 5% sodium hypochlorite solution (Sigma-Aldrich) for 10 s, and rinsed 3 times with ultrapure H_2O (Fresenius; Ibrahim et al. 2019). Finally, specimens were softly air-dried for 1 h semicovered and transferred immediately to the microscope.

Determination of MGO-Derived AGE Content in Dentin by ELISA

For the preparation of dentin tissue lysates, dentin sections were crushed into 1.5-mL Eppendorf tubes with the aid of pellet pestles (Sigma) and fully demineralized in a solution of 0.5M EDTA in 50mM Tris buffer (pH 7.4) for 72 h at 4 °C on an orbital shaker (Shinno et al. 2016). Protein content was measured with BCA assay, and samples were normalized to the same concentration in EDTA Tris buffer and diluted to 100 µg/mL of total protein with 0.1% BSA in PBS.

The presence of MGO-derived protein adducts was measured in the organic matrix of dentin by using a competitive ELISA (Abcam) according to manufacturer's instruction. Briefly, protein-binding 96-well plates were coated with 100 µL of 500-ng/mL MGO conjugate in PBS and incubated over night at 4 °C. Plates were then washed with assay wash buffer, blocked with assay diluent for 1 h at room temperature, and washed again. Wells were incubated with specimen or assay standard (50 µL) for 10 min, and 1× anti-MGO antibody (50 µL) was subsequently added. After 1-h incubation on an orbital shaker at room temperature, wells were washed and incubated with secondary antibody (HRP conjugated). Finally, the assay was developed with substrate solution (R&D Systems) for 20 min, and the reaction was stopped with 1M H_2SO_4 and analyzed with a microplate reader (Sunrise; Tecan).

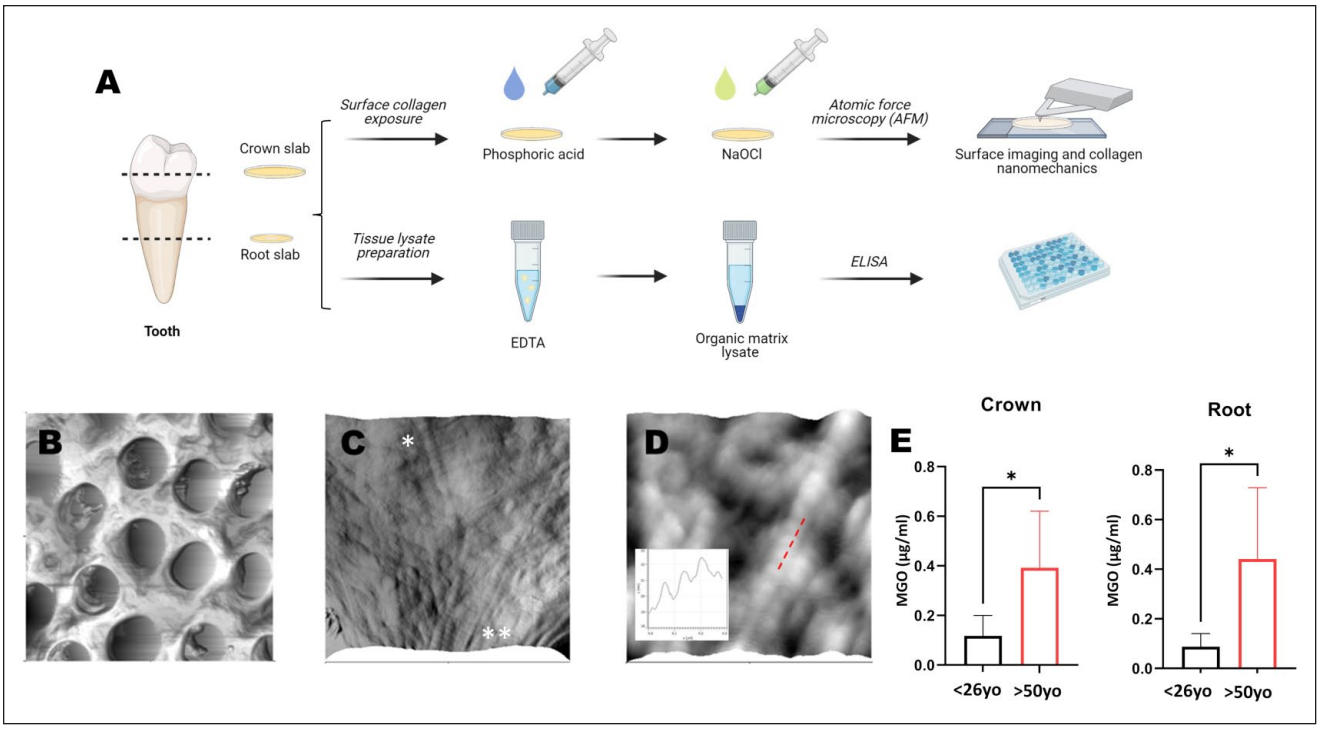

Figure 1. Study design and quantification of MGO-derived AGEs in human dentin. (**A**) Overview of tooth specimen preparation for AFM characterization and MGO-derived AGE quantification. Crown and root dentinal specimens from each tooth were processed for AFM and ELISA analysis. (**B**) AFM 3D reconstruction (20 × 20 µm; from height channel) of crown dentin following surface demineralization protocol, displaying characteristic dentinal tubules. (**C**) AFM 3D reconstruction (2.5 × 2.5 µm) of exposed intertubular (*) and peritubular (**) collagen fibrils. (**D**) AFM 3D reconstruction (1 × 1 µm) confirms the ultrastructure of collagen represented by regular D-banding periodicity. Inset: collagen fibril profile from area marked with red line. (**E**) MGO-derived AGE quantification from the organic matrix of demineralized dentin from the crown and root of patients <26 y and >50 y old shows an increase in MGO content in older specimens ($n = 6$). Values are presented as mean ± SD. *$P < 0.05$, *t* test. 3D, 3-dimensional; AFM, atomic force microscopy; AGE, advanced glycation end product; MGO, methylglyoxal. This figure is available in color online.

AFM Imaging and Nanomechanical Characterization of Dentinal Collagen

For this investigation, all AFM experiments were carried out with an MFP 3D-SA (Asylum Research) utilizing TAP300GD-G cantilevers ($k \approx 24$ N/m; BudgetSensors). Dentinal specimens were attached to magnetic microscopy discs with double-sided tape, and height and amplitude channel images of substrates were obtained in intermittent contact mode in air. Each cantilever was calibrated before experimentation via proprietary software, and a minimum of 3 scans (5 × 5 µm, 256 × 256 pixels) was obtained on representative areas of each specimen. Following topographic imaging, force-distance curves were obtained on individualized collagen fibrils by employing an adaptation of a previously published approach (Ibrahim et al. 2019). Briefly, collagen fibrils were indented with a maximum loading force of 30 nN and a constant loading speed along the center of each fibril in the dentinal regions: peritubular (PT; circumferential fibrils surrounding the tubule) and intertubular (IT; fibrils between tubules). A total of 100 force-distance curves were obtained per image (50 PT + 50 IT) for a total of 300 curves across the 3 areas of each specimen. From the resulting force-distance curves, dentinal collagen Young's moduli (YM) were calculated through the DMT model (Derjaguin, Muller, and Toporov) in proprietary AFM software (version 16.10.211 [Asylum Research]; Schuh et al. 2021).

Principal Component Analysis

Principal component analysis (PCA) was carried out to understand the association among all studied nanomechanical and molecular variables in coronal and root dentin among all patients (Jolliffe and Cadima 2016). For this analysis, all values for MGO concentrations and collagen elasticity in PT and IT regions for each patient were considered independent variables. The PCA was also performed on the <26-y-old and >50-y-old groups separately for better data visualization. From all variables, 5 principal components (PCs) were generated and selected per the Kaiser rule (PCs with eigenvalues >1.0). The loading plot of the first and second PCs of each group was generated and compared for <26-y-olds versus >50-y-olds and crown versus root groups with Origin Pro 2018 (OriginLab Corporation). Score plots were obtained with Prism 9 software (GraphPad).

Statistical Analysis

All data were tabulated and analyzed with Prism 9. After outlier detection, statistical significance was assessed with linear

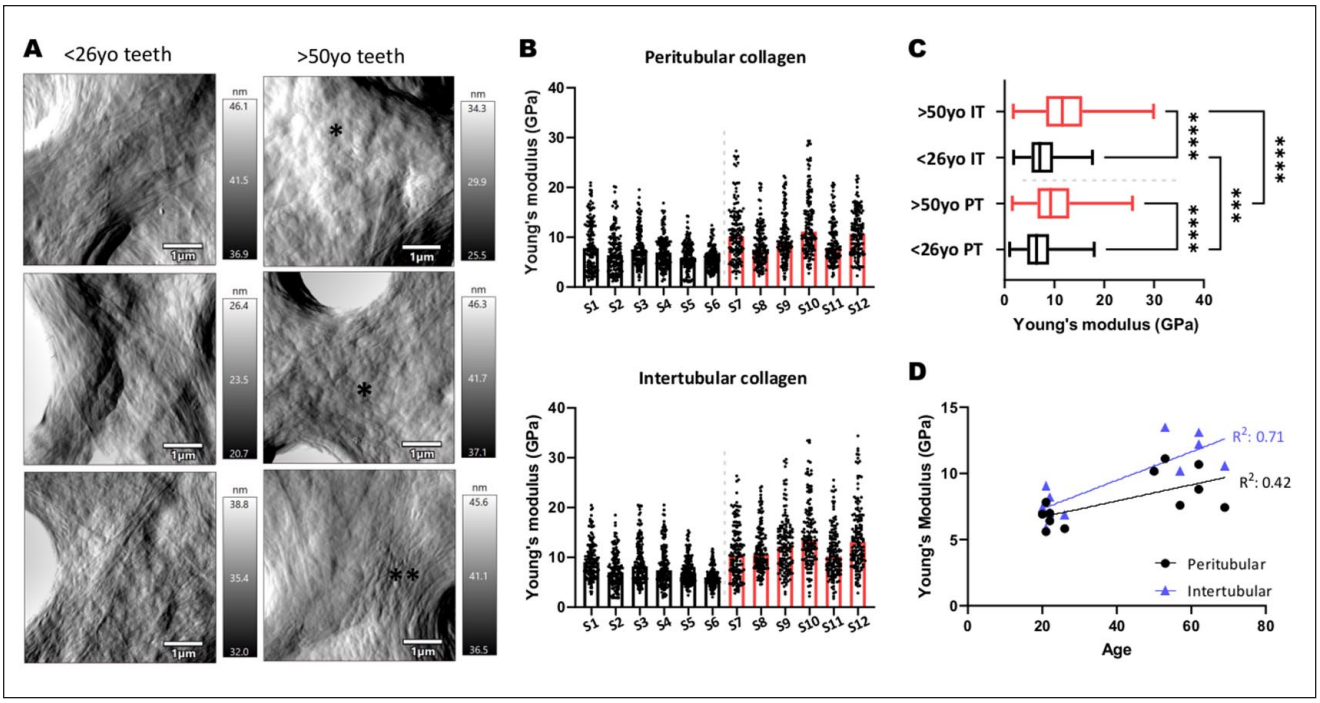

Figure 2. Ultrastructural and nanomechanical characterization of PT and IT collagen in coronal human dentin. (**A**) Representative AFM amplitude images of the dentinal organic matrix in young and aged teeth, displaying PT and IT collagen. Asterisks indicate areas with loss of fibril register (*) and fibril wrinkling (**). (**B**) Collagen fibril YM for each examined tooth in the PT and IT regions ($n = 150$ force-distance curves per region). Bars represent medians. (**C**) Pooled YM collagen elasticity values for the <26-y-old and >50-y-old groups in the PT and IT regions. ***$P < 0.001$. ****$P < 0.0001$. Kruskal-Wallis test. Values are presented as median (line), interquartile range (box), and min-max (error bars) (**D**) Linear regression plotted for tooth age vs YM for PT and IT collagen fibrils. AFM, atomic force microscopy; IT, intertubular; PT, peritubular; YM, Young's moduli.

regression, a *t* test, or a Kruskal-Wallis test, considering a significance value of $P < 0.05$. Elasticity values are expressed as median with 95% CI.

Results

By utilizing an adaptation of a previously published approach, it was possible to obtain dentinal sections from the tooth specimens of patients <26 y old ($n = 6$; mean ± SD age, 22 ± 2.1 y) and >50 y old ($n = 6$, 58 ± 6.9 y) from which the organic matrix was exposed (Ibrahim et al. 2019; Fig. 1B). In all cases, the exposure of dentinal collagen was reproducible and preserved the native appearance of fibrillar collagen, displaying its characteristic morphologic markers including D-banding periodicity (Fig. 1C, D; Appendix Figs. 1 and 2).

To determine the age-dependent accumulation of MGO-derived AGEs in the organic matrix of crown and root dentin, dentinal sections were demineralized with an EDTA solution and assessed with competitive ELISA. In crown and root dentin (Fig. 1E), we found a significant increase of MGO-derived AGEs in the >50-y-old group (crown, 0.39 ± 0.23 µg/mL; root, 0.44 ± 0.28 µg/mL) as compared with <26-y-old patients (crown, 0.12 ± 0.08 µg/mL; root, 0.09 ± 0.05 µg/mL; $P < 0.05$, normalized to total protein).

Subsequent imaging of the coronal dentinal collagen matrix with intermittent contact AFM across all 6 specimens <26 y old demonstrated the presence of collagen fibrils throughout the PT and IT regions with a clear D-banding register (Fig. 2A). Nanomechanical analysis of PT collagen fibrils in the <26-y-old group showed YM mostly in the <10-GPa range (Fig. 2B), with a median of 6.43 GPa (95% CI, 6.25 to 6.77) across all 6 specimens. In the >50-y-old group (Fig. 2C), however, there was a significant increase in PT collagen elasticity to a median of 9.25 GPa (95% CI, 8.73 to 9.73; $P < 0.0001$, Kruskal-Wallis test). IT collagen also had higher YM than PT collagen in both age groups ($P < 0.0001$, Kruskal-Wallis test), and the mechanical properties of IT collagen similarly varied as a function of age: 7.09 GPa (95% CI, 6.86 to 7.39) and 11.59 GPa (95% CI, 11.2 to 12.06) for the <26-y-old and >50-y-old groups, respectively. The age-associated increase in elasticity follows a linear trend for PT ($P < 0.05$) and IT ($P < 0.001$) collagen (Fig. 2D). These data suggest that AGE accumulation in the collagen matrix of dentin is not exclusive to the PT region, as IT collagen increases its YM as a function of age. The <26-y-old group displayed a very homogeneous grouping of YM for PT (interquartile range [IQR] = 4.35) and IT (IQR = 4.27), which spread across a wider range of values in the >50-y-old group (IQR = 6.37 and 7.24 for PT and IT, respectively). This observation suggests that despite an increase in YM, there are important individual variations regarding the aging process of dentinal collagen among patients.

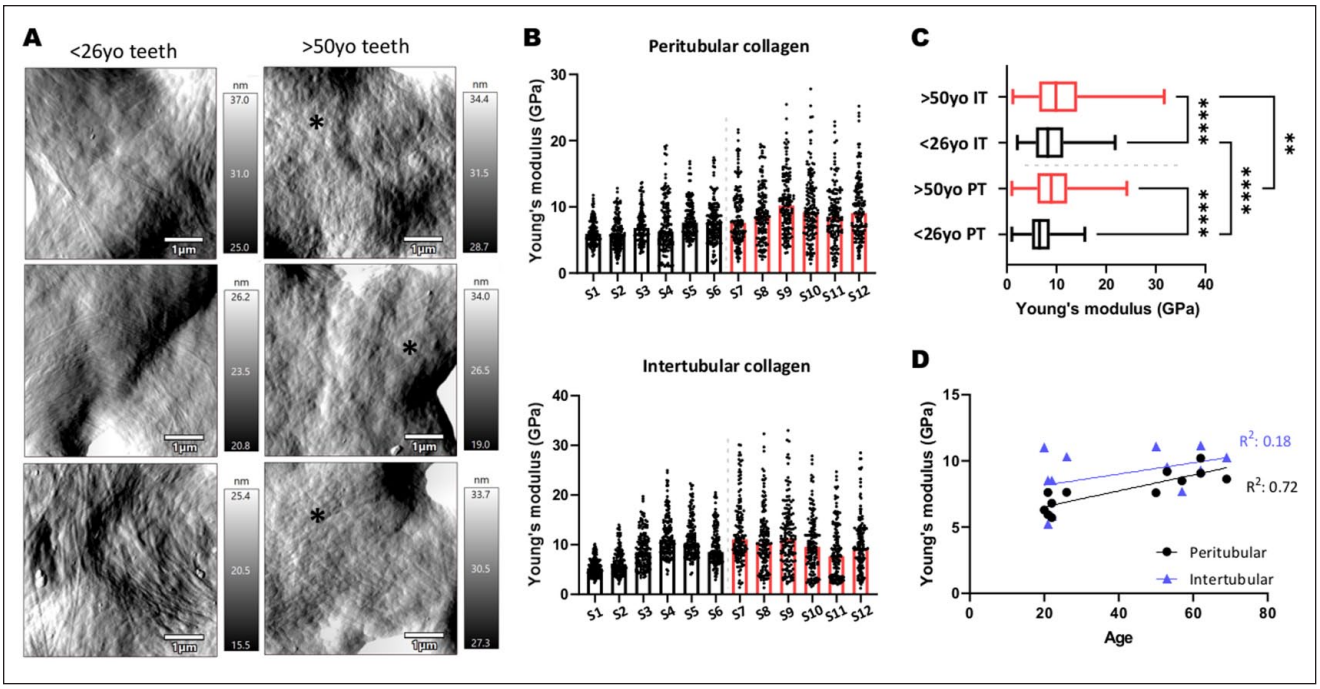

Figure 3. Ultrastructural and nanomechanical characterization of PT and IT collagen in radicular human dentin. (**A**) Representative AFM amplitude images of the dentinal organic matrix in young and aged teeth, displaying PT and IT collagen. Asterisk indicates area with loss of fibril register (*). (**B**) Collagen fibril YM for each examined tooth in the PT and IT regions ($n = 150$ force-distance curves per region). Bars represent medians. (**C**) Pooled YM collagen elasticity values for the <26-y-old and >50-y-old groups in PT and IT regions of root dentin slabs. **$P<0.01$. ****$P<0.0001$. Kruskal-Wallis test. Values are presented as median (line), interquartile range (box), and min-max (error bars) (**D**) Linear regression plotted for tooth age vs YM for PT and IT collagen fibrils in the root portion of each tooth. AFM, atomic force microscopy; IT, intertubular; PT, peritubular; YM, Young's moduli.

Root sections were prepared and analyzed by AFM with the same approach. Similar to crown dentin, fibrillar collagen was observed in root dentin from <26-y-old specimens and organized in PT and IT areas. Ultrastructure of collagen in the >50-y-old group included diverse areas with a lack of register and a loss of clear fibril morphology (Fig. 3A). These morphologic changes were accompanied by an increase in YM for PT and IT in the >50-y-old group versus the <26-y-old group (Fig. 3B). The median PT collagen elasticity values increased from 6.57 GPa (95% CI, 6.3 to 6.83) to 8.95 GPa (95% CI, 8.53 to 9.27; Fig. 3C), and median IT values increased from 8.25 GPa (95% CI, 7.99 to 8.54) to 9.87 GPa (95% CI, 9.47 to 10.37; $P<0.0001$, Kruskal-Wallis test). Similar to crown dentin, the modulus of elasticity of PT collagen increased linearly with age ($P<0.001$); however, the same association was not found for IT collagen, as it displayed higher heterogenicity in both groups (Fig. 3D).

As the final step, PCA was carried out to understand the association among all studied nanomechanical and molecular variables in coronal and root dentin. When MGO levels and IT and PT collagen nanomechanical properties were analyzed together, specimens showed clear clustering in 2 distinct groups distributed along the PC1 axis representing <26-y-old and >50-y-old patients, with no clear influence of patient sex (Fig. 4A). The intragroup variability among the <26-y-old specimens (blue dashed line) was reduced as compared with the >50-y-old specimens (green dashed line). Subsequent PCA analyses by location and age group were performed. In the crown, the mechanical properties of PT and IT collagen differed greatly between the <26-y-old and >50-y-old groups (Fig. 4B). In the root, the strongest difference among the <26-y-old and >50-y-old groups was given by the mechanical properties of IT collagen, which separated mostly along the PC1 axis (Fig. 4C). Furthermore, PCA was utilized to obtain profiles for the specimens <26 y old (Fig. 4D) and >50 y old (Fig. 4E). In younger patients, there were no clear differences between the mechanical properties of PT and IT collagen; however, the YM of collagen varied importantly between crown and root. A different pattern was observed in >50-y-old patients, where separation among specimens is mostly explained by differences in the mechanical properties of crown IT collagen.

Discussion

In this study we have characterized age-associated changes in the collagen matrix of human teeth utilizing an interdisciplinary nanomechanical approach. For all specimens, the exposure of dentinal collagen in permanent teeth was reproducible and preserved the native appearance of fibrillar collagen, displaying its characteristic morphologic markers including D-banding periodicity under the AFM (Fig. 1C, D) as previously observed (Habelitz et al. 2002; Fawzy et al. 2012). However, >50-y-old specimens showed a reduced presence of collagen fibrils and

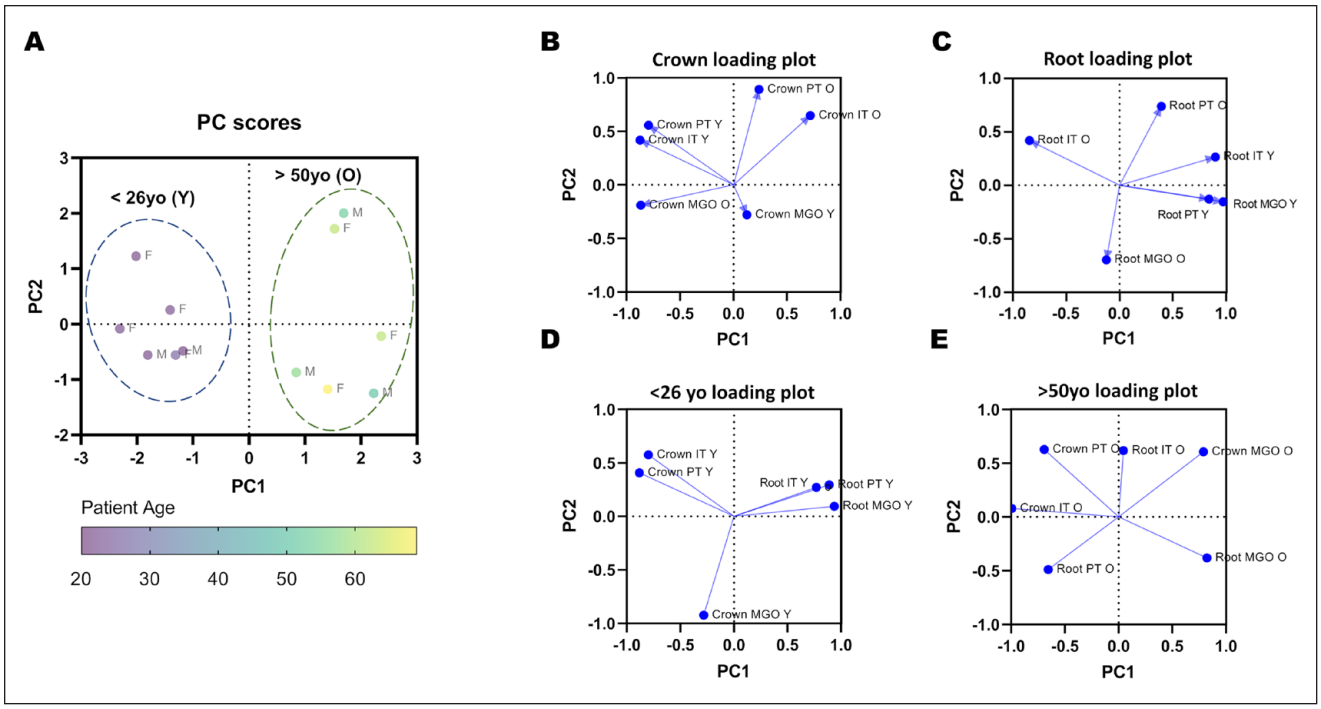

Figure 4. Principal component analysis of molecular and nanomechanical aging parameters in human dentin. (**A**) Score plot for all studied variables demonstrates clustering of specimens along the PC1 as a function of patient age in the <26-y-old group (younger patients; Y) and >50-y-old group (older patients; O). (**B**, **C**) Loading plots describe the association of all studied variables in crown and root dentin. (**D**, **E**) Loading plots describe the relationship of aging variables in the <26- and >50-y-old groups. IT, intertubular; MGO, methylglyoxal; PC, principal component; PT, peritubular.

an increase in areas of wrinkling and loss of register (Fig. 2A, asterisks), known to be representative of collagen aging in human tissues (Ahmed et al. 2017).

Previous research has shown that MGO-derived AGEs accumulate in the dental pulp and periodontal tissues (Retamal et al. 2016; Delle Monache et al. 2021); however, to date, no studies have investigated their presence in dentin. The present ELISA-based quantification suggests that, in fact, MGO-derived AGEs collect within the organic matrix of dentin over time. Unlike bone, dentin has no turnover, which facilitates the accumulation of AGEs in its organic matrix, similar to other slow turnover tissues such as tendons (Birch 2018). Recent work has demonstrated that the AGE pentosidine accumulates in dentin with aging (Shinno et al. 2016; Greis et al. 2018) and the AGE N-carboxymethyl lysine accumulates in dentinal collagen and increases mechanical resistance (Miura et al. 2014). This accumulation of AGEs in dentin could be explained by the constant perfusion of dentinal fluid—a serum-derived fluid—from the dental pulp into the tubules over time. Despite the presence of amorphous proteins (Ravindran and George 2015), the organic matrix of dentin is predominantly composed of collagen (specifically type I collagen; Goldberg 2011), which functions as the main target for MGO and other AGE modification.

In this report, we have observed that aging leads to an increase in the elastic modulus of dentinal collagen, associated with higher MGO levels in the organic matrix. The distribution of collagen modulus data is consistent with previous reports and reflects the biological variability of complex tissue samples (Manssor et al. 2016; Calò et al. 2020). Indeed, AGE accumulation has been shown to increase the YM of collagen in tissue and in vitro experiments (Verzijl et al. 2002; Depalle et al. 2015; Panwar et al. 2015; Schuh et al. 2021), suggesting that the increase in elasticity observed in PT and IT collagen is mediated by the accumulation of MGO adducts and other potential AGEs and crosslinks (Lederer and Bühler 1999). In root dentin, the observed nanomechanical values for dentinal collagen are similar to those reported by Ho et al. (2007) in demineralized cementum (4 to 7 GPa).

As the final step, PCA was carried out to understand the association among all studied variables. PCA is a statistical method that reduces a determined number of intercorrelated variables into dimensionless parameters called *principal components* (Jolliffe and Cadima 2016), and it has been recently used in dentistry to facilitate the interpretation of complex data sets (da Fontoura et al. 2015; Elbahary et al. 2020). The result of our PCA suggests that nanomechanical changes and MGO accumulation in the organic matrix of coronal dentin are important markers for tooth aging. Furthermore, different "aging profiles" for crown and root dentinal collagen were observed, which could have important therapeutic implications in restorative and adhesive dentistry approaches. Our results suggest that mechanical changes in collagen associated with aging are widespread throughout dentin, involving PT and IT collagen in crown and root. These distinctive nanomechanical and molecular profiles observed in >50-y-old specimens strengthen the importance of understanding how the process of aging affects

the mechanical properties of dentinal collagen. These aging-associated collagen changes may have important repercussions for restorative dentistry approaches, such as adhesive bonding to dentin and hybrid layer formation (Breschi et al. 2018), bacterial adhesion and degradation during dentinal and root caries progression (Schuh et al. 2021; Álvarez et al. 2021), and root caries restoration in the elderly. Finally, the role of AGE-promoting diseases such as diabetes on dentinal collagen mechanobiology should be explored in future.

Conclusions

An increase in dentinal MGO was observed in >50-y-old versus <26-y-old patients in crown and root. AFM nanoscale characterization demonstrated morphologic alterations in the organic matrix of >50-y-old crown dentin specimens, including loss of collagen ultrastructure and fibril banding. Furthermore, higher YM values in PT and IT collagen fibrils were found in the >50-y-old group, which increased linearly with age. Similarly, root-derived dentinal specimens displayed morphologic changes and an increase in collagen fibril modulus of elasticity in the >50-y-old group, which was more pronounced in PT collagen. Finally, PCA showed the formation of 2 clusters among specimens from similar age groups that was mostly determined by differences in PT and IT crown elasticity as well as MGO-derived AGE formation in crown dentin. Within each age group, variability was mostly given by differences in the elastic behavior of IT collagen in root dentin. These results demonstrate that human dentinal collagen matrix undergoes important age-related nanomechanical changes, with a potential impact on restorative dentistry approaches and dentinal biofilm formation in the elderly.

Author Contributions

C.M.A.P. Schuh, contributed to design, data acquisition, analysis, and interpretation, drafted and critically revised the manuscript; C. Leiva-Sabadini, S. Huang, contributed to data analysis and interpretation, critically revised the manuscript; N.P. Barrera, contributed to design and data interpretation, critically revised the manuscript; L. Bozec, contributed to design, data analysis, and interpretation, critically revised the manuscript; S. Aguayo, contributed to conception, design, data acquisition, analysis, and interpretation, drafted and critically revised the manuscript. All authors gave final approval and agree to be accountable for all aspects of the work.

Acknowledgments

Figure 1A was created with Biorender.com. The authors thank Camila Ramos and Dr. Gonzalo Narea for their support with tooth sample collection. This work was previously posted on MedRXiv(https://www.medrxiv.org/content/10.1101/2021.08.31.21262730v1).

Declaration of Conflicting Interests

The authors declared no potential conflicts of interest with respect to the research, authorship, and/or publication of this article.

Funding

The authors disclosed receipt of the following financial support for the research, authorship, and/or publication of this article: This work was supported by the ANID FONDECYT Iniciación Grant 11180101 and Millennium Science Initiative P10-035F.

ORCID iDs

C.M.A.P. Schuh https://orcid.org/0000-0001-9475-4513
S. Aguayo https://orcid.org/0000-0003-0900-1993

References

Ahmed T, Nash A, Clark KE, Ghibaudo M, de Leeuw NH, Potter A, Stratton R, Birch HL, Enea Casse R, Bozec L. 2017. Combining nano-physical and computational investigations to understand the nature of "aging" in dermal collagen. Int J Nanomedicine. 12:3303–3314.

Álvarez S, Leiva-Sabadini C, Schuh CMAP, Aguayo S. 2021. Bacterial adhesion to collagens: implications for biofilm formation and disease progression in the oral cavity. Crit Rev Microbiol [epub ahead of print 16 Jul 2021] in press. doi:10.1080/1040841X.2021.1944054

Birch HL. 2018. Extracellular matrix and ageing. In: Harris JR, Korolchuk VI, editors. Biochemistry and cell biology of ageing: part I biomedical science. Singapore: Springer Singapore. p. 169–190.

Breschi L, Maravic T, Cunha SR, Comba A, Cadenaro M, Tjäderhane L, Pashley DH, Tay FR, Mazzoni A. 2018. Dentin bonding systems: from dentin collagen structure to bond preservation and clinical applications. Dent Mater. 34(1):78–96.

Calò A, Romin Y, Srouji R, Zambirinis CP, Fan N, Santella A, Feng E, Fujisawa S, Turkekul M, Huang S, et al. 2020. Spatial mapping of the collagen distribution in human and mouse tissues by force volume atomic force microscopy. Sci Rep. 10(1):15664.

Capella-Monsonís H, Coentro JQ, Graceffa V, Wu Z, Zeugolis DI. 2018. An experimental toolbox for characterization of mammalian collagen type I in biological specimens. Nat Protoc. 13(3):507–529.

da Fontoura CSG, Miller SF, Wehby GL, Amendt BA, Holton NE, Southard TE, Allareddy V, Moreno Uribe LM. 2015. Candidate gene analyses of skeletal variation in malocclusion. J Dent Res. 94(7):913–920.

Delle Monache S, Pulcini F, Frosini R, Mattei V, Talesa VN, Antognelli C. 2021. Methylglyoxal-dependent glycative stress is prevented by the natural antioxidant oleuropein in human dental pulp stem cells through Nrf2/Glo1 pathway. Antioxidants. 10(5):716.

Depalle B, Qin Z, Shefelbine SJ, Buehler MJ. 2015. Influence of cross-link structure, density and mechanical properties in the mesoscale deformation mechanisms of collagen fibrils. J Mech Behav Biomed Mater. 52:1–13.

DiLoreto R, Murphy CT. 2015. The cell biology of aging. Mol Biol Cell. 26(25):4524–4531.

Dufrêne YF, Viljoen A, Mignolet J, Mathelié-Guinlet M. 2021. AFM in cellular and molecular microbiology. Cell Microbiol. 23(7):e13324.

Elbahary S, Haj-yahya S, Khawalid M, Tsesis I, Rosen E, Habashi W, Pokhojaev A, Sarig R. 2020. Effects of different irrigation protocols on dentin surfaces as revealed through quantitative 3D surface texture analysis. Sci Rep. 10(1):22073.

Fawzy A, Nitisusanta L, Iqbal K, Daood U, Beng LT, Neo J. 2012. Characterization of riboflavin-modified dentin collagen matrix. J Dent Res. 91(11):1049–1054.

Fessel G, Li Y, Diederich V, Guizar-Sicairos M, Schneider P, Sell DR, Monnier VM, Snedeker JG. 2014. Advanced glycation end-products reduce collagen molecular sliding to affect collagen fibril damage mechanisms but not stiffness. PLoS One. 9(11):e110948.

Gkogkolou P, Böhm M. 2012. Advanced glycation end products: key players in skin aging? Dermatoendocrinol. 4(3):259–270.

Goldberg M. 2011. Dentin structure composition and mineralization. Front Biosci. 3:711–735.

Greis F, Reckert A, Fischer K, Ritz-Timme S. 2018. Analysis of advanced glycation end products (AGEs) in dentine: useful for age estimation? Int J Legal Med. 132(3):799–805.

Gurav AN. 2013. Advanced glycation end products: a link between periodontitis and diabetes mellitus? Curr Diabetes Rev. 9(5):355–361.

Habelitz S, Balooch M, Marshall SJ, Balooch G, Marshall GW. 2002. In situ atomic force microscopy of partially demineralized human dentin collagen fibrils. J Struct Biol. 138(3):227–236.

Ho SP, Marshall SJ, Ryder MI, Marshall GW. 2007. The tooth attachment mechanism defined by structure, chemical composition and mechanical properties of collagen fibers in the periodontium. Biomaterials. 28(35):5238–5245.

Ibrahim S, Strange AP, Aguayo S, Parekh S, Bozec L. 2019. Phenotypic properties of collagen in dentinogenesis imperfecta associated with osteogenesis imperfecta. Int J Nanomedicine. 14:9423–9435.

Jolliffe IT, Cadima J. 2016. Principal component analysis: a review and recent developments. Philos Trans R Soc A Math Phys Eng Sci. 374(2065): 20150202.

Lederer MO, Bühler HP. 1999. Cross-linking of proteins by maillard processes—characterization and detection of a lysine-arginine cross-link derived from D-glucose. Bioorg Med Chem. 7(6):1081–1088.

Manssor NAS, Radzi Z, Yahya NA, Mohamad Yusof L, Hariri F, Khairuddin NH, Abu Kasim NH, Czernuszka JT. 2016. Characteristics and Young's modulus of collagen fibrils from expanded skin using anisotropic controlled rate self-inflating tissue expander. Skin Pharmacol Physiol. 29(2):55–62.

Miura J, Nishikawa K, Kubo M, Fukushima S, Hashimoto M, Takeshige F, Araki T. 2014. Accumulation of advanced glycation end-products in human dentine. Arch Oral Biol. 59(2):119–124.

Murray Thomson W. 2014. Epidemiology of oral health conditions in older people. Gerodontology. 31 Suppl 1:9–16.

Nass N, Bartling B, Santos AN, Scheubel RJ, Börgermann J, Silber RE, Simm A. 2007. Advanced glycation end products, diabetes and ageing. Z Gerontol Geriatr. 40(5):349–356.

Panwar P, Lamour G, Mackenzie NCW, Yang H, Ko F, Li H, Brömme D. 2015. Changes in structural-mechanical properties and degradability of collagen during aging-associated modifications. J Biol Chem. 290(38):23291–23306.

Poundarik AA, Wu P-C, Evis Z, Sroga GE, Ural A, Rubin M, Vashishth D. 2015. A direct role of collagen glycation in bone fracture. J Mech Behav Biomed Mater. 52:120–130.

Prince MJ, Wu F, Guo Y, Gutierrez Robledo LM, O'Donnell M, Sullivan R, Yusuf S. 2015. The burden of disease in older people and implications for health policy and practice. Lancet. 385(9967):549–562.

Qian L, Zhao H. 2018. Nanoindentation of soft biological materials. Micromachines. 9(12):654.

Ravindran S, George A. 2015. Dentin matrix proteins in bone tissue engineering. Adv Exp Med Biol. 881:129–142.

Retamal IN, Hernández R, González-Rivas C, Cáceres M, Arancibia R, Romero A, Martínez C, Tobar N, Martínez J, Smith PC. 2016. Methylglyoxal and methylglyoxal-modified collagen as inducers of cellular injury in gingival connective tissue cells. J Periodontal Res. 51(6):812–821.

Schuh CMAP, Benso B, Naulin PA, Barrera NP, Bozec L, Aguayo S. 2021. Modulatory effect of glycated collagen on oral streptococcal nanoadhesion. J Dent Res. 100(1):82–89.

Shinno Y, Ishimoto T, Saito M, Uemura R, Arino M, Marumo K, Nakano T, Hayashi M. 2016. Comprehensive analyses of how tubule occlusion and advanced glycation end-products diminish strength of aged dentin. Sci Rep. 6:19849.

Snedeker JG, Gautieri A. 2014. The role of collagen crosslinks in ageing and diabetes—the good, the bad, and the ugly. Muscles Ligaments Tendons J. 4(3):303–308.

Strange AP, Aguayo S, Ahmed T, Mordan N, Stratton R, Porter SR, Parekh S, Bozec L. 2017. Quantitative nanohistological investigation of scleroderma: an atomic force microscopy-based approach to disease characterization. Int J Nanomedicine. 12:411–420.

Sui BD, Hu CH, Zheng CX, Jin Y. 2016. Microenvironmental views on mesenchymal stem cell differentiation in aging. J Dent Res. 95(12): 1333–1340.

Verzijl N, DeGroot J, Zaken CB, Braun-Benjamin O, Maroudas A, Bank RA, Mizrahi J, Schalkwijk CG, Thorpe SR, Baynes JW, et al. 2002. Crosslinking by advanced glycation end products increases the stiffness of the collagen network in human articular cartilage: a possible mechanism through which age is a risk factor for osteoarthritis. Arthritis Rheum. 46(1):114–123.

Wetzels S, Wouters K, Schalkwijk CG, Vanmierlo T, Hendriks JJA. 2017. Methylglyoxal-derived advanced glycation endproducts in multiple sclerosis. Int J Mol Sci. 18(2):421.